PROCEEDINGS OF SCIENCE

Comprehensive comparison of radio emission predicted by CoREAS and ZHAireS.

Carlo Salvattore Cruz Sanchez,[a,*] **Patricia M. Hansen,**[a,b] **Jaime Alvarez Muñiz,**[c] **Matias Tueros**[a] **and Diego Gabriel Melo**[d]

[a] *IFLP (CCT La Plata-CONICET),*
Departamento de Física, Fac. de Cs. Exactas, UNLP;
Universidad Nacional de La Plata, C. C. 67 - 1900 La Plata, Argentina.
[b] *Departamento de Ciencias Básicas, Facultad de Ingeniería, UNLP;*
Universidad Nacional de La Plata, C. C. 67 - 1900 La Plata, Argentina.
[c] *Instituto Galego de Física de altas Enerxías IGFAE;*
Universidade de Santiago de Compostela, Spain.
[d] *ITeDA (CNEA - CONICET - UNSAM),*
CAC - CNEA, Av. Gral Paz 1499;
(1650) San Martín - Buenos Aires - Argentina.
E-mail: carlo.cruz@iflp.unlp.edu.ar, patricia.hansen@ing.unlp.edu.ar, tueros@fisica.unlp.edu.ar, jaime.alvarez@usc.es, diego.melo@iteda.cnea.gov.ar

Radio detection of cosmic-ray induced extended air showers (EAS) has undergone an impressive development in the last two decades. Several ultra-high energy cosmic ray experiments are routinely detecting radio pulses in the MHz to GHz frequency range from EAS. These experimental developments require precise knowledge of the properties of the emitted radiation in order to interpret and analyze the collected data. We present a comparison of predicted radio pulses emitted by EAS simulated with CoREAS and ZHAireS, the two main and most widely used Monte Carlo simulation packages for this purpose. We have performed a set of simulations of the radio emission in EAS induced by different primary particles, shower directions and magnetic field configurations. We have compared the frequency spectrum of the electric field amplitude on the ground predicted by both packages at various observer positions with respect to the shower axis. We have used in both simulations input parameters as similar as possible, as well as a similar realistic atmospheric refractive index as a function of altitude. In addition, we have compared showers with very similar values of depth of shower maximum. We have found a very good agreement, with typical relative differences of less than 10%, between the CoREAS and ZHAireS predictions for the dominant components of the electric field in the frequency range from a few MHz to hundreds of MHz, where most experiments exploiting the radio technique for EAS detection operate.

38th International Cosmic Ray Conference (ICRC2023)
26 July - 3 August, 2023
Nagoya, Japan

*Speaker

PoS(ICRC2023)290

1. Introduction

Ultra-high-energy cosmic rays (UHECRs) are particles with energies around and above the EeV range. As these particles interact with the upper layers of Earth's atmosphere, they initiate extensive air showers (EAS) composed of secondary particles. Understanding the properties of EAS is crucial for unraveling the nature and origin of UHECRs. To investigate EAS, multiple detection methods are utilized. Arrays of surface detectors sample the shower front on the ground, allowing for measurements of particle densities and arrival times. Fluorescence detectors capture the fluorescence light produced by UHECR interactions in the atmosphere, providing longitudinal information about the showers. In addition to these techniques, radio detection is an invaluable tool due to the minimal atmospheric absorption experienced by radio signals and the richness of information on the shower that can be obtained [1]. It has been demonstrated that the shower energy and the depth of the shower maximum can be accurately determined using radio detection with an almost 100% duty cycle of operation.

The emission of radio signals in EAS arises from two main mechanisms: the geomagnetic effect and the Askaryan mechanism. The geomagnetic effect consists of a drift current due to charge separation in the magnetic field $\vec{B}$, inducing a polarization pattern that is approximately parallel to $-\hat{v} \times \vec{B}$ (i.e., along the direction of the Lorentz force), where $\hat{v}$ represents the direction of the shower axis. The intensity of the geomagnetically-induced field is proportional to the magnitude of the magnetic field $|\vec{B}|$ and the sine of the geomagnetic angle α, which is the angle between $\hat{v}$ and $\vec{B}$. On the other hand, the Askaryan mechanism is attributed to the excess of electrons over positrons in the shower, induced by particle physics processes such as Compton, Möller, Bhabha scatterings, and electron-positron annihilation. The Askaryan mechanism results in a polarization perpendicular to the direction $\hat{u} \times (\hat{u} \times \hat{v})$, where $\hat{u}$ is a unit vector from the emission point to the observer.

The accurate interpretation of data obtained from experiments utilizing the radio technique relies on precise simulations of the radio pulses generated in extensive air showers (EAS). The two main Monte Carlo simulation programs used for this purpose are CoREAS [2] and ZHAireS [3]. In both programs, charged particles are tracked with different approximations, and the electric field induced by each particle is obtained by solving Maxwell's equations using different computational algorithms. These calculations are based on first principles of electromagnetism and do not assume any *a priori* emission mechanism or involve any free parameters. Simulations performed with ZHAireS and CoREAS have shown consistent results between themselves [4] and when compared to data [5, 6]. However, the comparisons between the two programs have been limited to a specific number of shower geometries [4], a restricted frequency range [7, 8], or a limited number of observables such as the energy radiated in the form of radio waves [7]. While a good level of agreement has been achieved between the predictions of CoREAS and ZHAireS [4], a more comprehensive comparison of the results of the two programs is currently lacking. This includes studying a wider range of shower geometries, primary particle types, and selecting showers simulated under similar conditions, including those with a similar penetration in the atmosphere. The aim of this work is to fill these gaps and provide a more thorough comparison between the predictions of CoREAS and ZHAireS

2. Monte Carlo Simulation of Radio emission in EAS

As previously mentioned, the two most commonly used radio simulation programs for modeling the radio signals produced in extensive air showers (EAS) are CoREAS and ZHAireS.

2.1 CoREAS

CoREAS [2] is a cutting-edge Monte Carlo program specifically designed for simulating radio emission from EAS. The simulation of the shower development in the atmosphere is performed using CORSIKA [9], which provides information about the type, energy, time, and position of each tracked particle. This particle

data is then utilized in CoREAS to calculate the electric field contribution through the use of the *endpoints algorithm* based on fundamental principles of electromagnetism. The endpoints algorithm describes particle motion along a trajectory using discrete instantaneous acceleration and deceleration events, which are associated with the production of radiation. In CoREAS, the simulation takes into account the effects of the atmospheric refractive index, that is greater than 1 and varies with altitude. The program allows users to choose different models for the atmospheric refractive index, as explained in the following section. For our simulations in this study, we utilized CORSIKA 7.7410 and CoREAS V1.4. Additional details can be found in the respective user's manuals [10, 11].

2.2 ZHAireS

The other leading program for calculating radio emission in EAS is ZHAireS [3]. In ZHAireS, the AIRES shower simulation program [12] is used to propagate each particle in small steps that are regarded as single particle tracks. Their contribution to the radio emission is calculated and added to the total electric field in both the time [13] and frequency domains [14] applying the *ZHS algorithm* developed by Zas-Halzen-Stanev and originally implemented in the ZHS program [14, 13]. This algorithm is also obtained from first principles solving Maxwell's equations. In the ZHS expression for the electric field, there are two terms for each sub-track corresponding to the start and the end points. In this respect, the methodology is similar to the endpoints one but a practical difference is that in the ZHS algorithm the attenuation of the electric field with distance R^{-1} that is applied to the two terms in the expression for a sub-track is the same, while in the endpoints formulation a different value of R is independently calculated for each acceleration endpoint. In the limit of large R, the difference between the two approaches vanishes, but for sub-tracks that are not short compared to R, there can be numerical differences. More importantly, in the limit of observation angle with respect to the track close to the Cherenkov angle, θ_C, only in the ZHS approach the correct and finite limit can be taken [15]. As a result, the shower simulation programs that implement the endpoints algorithm such as CoREAS, require the use of the ZHS expressions for sub-tracks that are seen by observers very close to the Cherenkov angle. In ZHAireS, the variation with altitude of the atmospheric refractive index is modeled by default with an exponential function but also other models similar to those employed in CoREAS can be chosen as explained in the next section. We have used AIRES 19.04.08 and ZHAireS 1.0.30a for the simulations in this work. See their respective user's manuals for further details [16, 17].

3. Parameters of the CoREAS and ZHAireS simulations

We performed simulations comparing CoREAS and ZHAireS for various primary particles, shower geometries, and magnetic field configurations specified in our results. Many settings of the simulations such as energy thresholds of the particles, have been chosen to minimize the differences that can arise from shower development. Also, the primary particle, shower geometry and hadronic interaction model chosen in the simulations are the same when performing the comparisons.

Atmospheric refractive index. ZHAireS and CoREAS take into account the fact that the atmospheric refractive index is larger than one, and decreases with altitude h above ground. In CoREAS the default option is to model the refractive index with the Gladstone-Dale law which assumes that $n(h)$ varies in proportion to the atmospheric density. This model uses as input the value of the refractive index at ground and the density profile of the atmosphere. The Gladstone-Dale law is also implemented in ZHAireS. However, by default, ZHAireS uses an exponential model for $n(h)$ that is parameterized in terms of the refractivity $\mathcal{R}(h)$, defined as $[n(h) - 1] \times 10^6$ and given by $\mathcal{R}(h) = \mathcal{R}_s \exp(-\mathcal{K}_r h)$, where $\mathcal{R}_s$ and $\mathcal{K}_r$ can be changed by the user. To

make the simulations as similar as possible we used the Gladstone-Dale law option in ZHAireS (denoted as ZHAireS-GD[1]).

To ensure precise comparisons between ZHAireS and CoREAS showers, we implemented a particular methodology to minimize intrinsic differences resulting from shower development and inherent shower-to-shower fluctuations. For a given CoREAS shower, we first simulated a set of showers using AIRES without including the calculation of radio emission. From this sample, we selected the AIRES shower that exhibited the most similar depth of shower maximum ($X_{\rm max}$) to the CoREAS shower under consideration. Once the AIRES shower was chosen, we performed a second AIRES simulation, this time with the calculation of radio emission enabled using ZHAireS. Importantly, turning on the radio emission calculation in ZHAireS does not modify the sequence of random numbers used in the simulation, ensuring the preservation of the initially selected $X_{\rm max}$ value. By following this methodology, our aim was to ensure that any observed differences between ZHAireS and CoREAS showers primarily arose from the specific calculation of radio emission, rather than from intrinsic fluctuations in shower development.

4. Results

In figures 1 and 2, we present the Fourier components of the electric field E_x, E_y, and E_z as a function of frequency, as predicted in CoREAS and ZHAireS simulations. These simulations use primary iron-induced showers as input with an energy of 10^{17} eV and zenith angles of 45^0 (figure 1) and 60^0 (figure 2). We chose a horizontal magnetic field of $|\vec{B}| = 50\mu$T parallel to ground and directed northward. There is a very good level of agreement between the Fourier spectra predicted by CoREAS and ZHAireS in the frequency range of approximately 1 MHz to 300 MHz for the dominant component of the electric field, naely the E_y component for the particular geometry chosen. The differences between the results of CoREAS and ZHAireS are within 5% in most cases and typically grow above $\sim$ 300 MHz, at which the emission is largely incoherent and sensitive to shower-to-shower fluctuations and to the thinning algorithm applied in the simulations which is different in CoREAS and ZHAireS.

In Figure 3, we present a comparison of the predicted emission from CoREAS and ZHAireS for inclined showers (proton at 10^{18} eV), with zenith angle $\theta = 70^\circ$ and 80°. In this case, we used a vertical magnetic field configuration with $|\vec{B}| = 50, \mu$T, oriented perpendicular to the ground and directed towards magnetic north. We focus on the dominant E_y component of the Fourier transform of the electric field at frequency 50 MHz, as a function of the distance from the shower core along the south-north and east-west directions. The results reveal a good agreement at the level of $\simeq$ 5% between the two simulation programs in the region where the electric field is highest. The agreement is in general slightly worse for observers closer to the shower axis than for observers farther away from it.

5. Conclusions

We have carried out an extensive analysis comparing the predictions of radio emission from EAS using the well-known state of the art Monte Carlo simulation packages, CoREAS and ZHAireS. The comparison covered various aspects such as different primary particles, shower directions, and magnetic field configurations. To ensure a fair comparison, we carefully controlled relevant parameters for radio emission, including the model of refractive index, energy thresholds of particles, position of $X_{\rm max}$ (shower maximum), magnetic field configuration, and shower geometry, ensuring they were the same in both simulations.

Our study revealed a very good level of agreement between the CoREAS and ZHAireS simulations. The differences between the two codes were typically below 10% in the dominant components of the electric field across a wide frequency range, from a few MHz to several hundred MHz. This frequency range corresponds

[1]The Gladstone-Dale (GD) model is not implemented in the publicly available version of ZHAireS. ZHAireS-GD is a special version used for the comparisons in this study and will be incorporated into a future release of the public version.

to the operational range of most ground arrays of antennas that utilize the radio technique for detecting extensive air showers.

Acknowledgments: This work is funded by Xunta de Galicia (CIGUS Network of Research Centers & Consolidación ED431C-2021/22 and ED431F-2022/15); MCIN/AEI PID2019-105544GB-I00 - Spain; European Union ERDF.

References

[1] Frank G. Schröder. "Radio detection of Cosmic-Ray Air Showers and High-Energy Neutrinos". In: *Prog. Part. Nucl. Phys.* 93 (2017), pp. 1–68. DOI: 10.1016/j.ppnp.2016.12.002. arXiv: 1607.08781 [astro-ph.IM].

[2] T. Huege, M. Ludwig, and C. W. James. "Simulating radio emission from air showers with CoREAS". In: *AIP Conf. Proc.* 1535.1 (2013). Ed. by Robert Lahmann et al., p. 128. DOI: 10.1063/1.4807534. arXiv: 1301.2132 [astro-ph.HE].

[3] Jaime Alvarez-Muniz, Washington R. Carvalho Jr., and Enrique Zas. "Monte Carlo simulations of radio pulses in atmospheric showers using ZHAireS". In: *Astropart. Phys.* 35 (2012), pp. 325–341. DOI: 10.1016/j.astropartphys.2011.10.005. arXiv: 1107.1189 [astro-ph.HE].

[4] T. Huege. "Theory and simulations of air shower radio emission". In: *AIP Conf. Proc.* 1535.1 (2013). Ed. by Robert Lahmann et al., p. 121. DOI: 10.1063/1.4807533. arXiv: 1301.2135 [astro-ph.HE].

[5] A. Nelles et al. "Measuring a Cherenkov ring in the radio emission from air showers at 110–190 MHz with LOFAR". In: *Astropart. Phys.* 65 (2015), pp. 11–21. DOI: 10.1016/j.astropartphys.2014.11.006. arXiv: 1411.6865 [astro-ph.IM].

[6] Alexander Aab et al. "Measurement of the Radiation Energy in the Radio Signal of Extensive Air Showers as a Universal Estimator of Cosmic-Ray Energy". In: *Phys. Rev. Lett.* 116.24 (2016), p. 241101. DOI: 10.1103/PhysRevLett.116.241101. arXiv: 1605.02564 [astro-ph.HE].

[7] Marvin Gottowik et al. "Determination of the absolute energy scale of extensive air showers via radio emission: systematic uncertainty of underlying first-principle calculations". In: *Astropart. Phys.* 103 (2018), pp. 87–93. DOI: 10.1016/j.astropartphys.2018.07.004. arXiv: 1712.07442 [astro-ph.HE].

[8] Brian Rauch. "Comparison of ZHAireS and CoREAS radio emission simulations in the Ultra-High Frequency Band". In: *33rd International Cosmic Ray Conference*. 2013, p. 0954.

[9] D. Heck et al. *CORSIKA: A Monte Carlo Code to Simulate Extensive Air Showers*. FZKA Report 6019, Forschungszentrum Karlsruhe (1998).

[10] D. Heck and T. Pierog. *Extensive Air Shower Simulation with CORSIKA: A User's Guide (Version 7.7420)*. https://www.iap.kit.edu/corsika/70.php.

[11] T. Huege. *CoREAS 1.4 User's Manual*. https://web.ikp.kit.edu/huege/downloads/coreas-manual.pdf.

[12] S. J. Sciutto. "The AIRES system for air shower simulations: An Update". In: *27th International Cosmic Ray Conference*. June 2001. arXiv: astro-ph/0106044.

[13] Jaime Alvarez-Muniz, Andres Romero-Wolf, and Enrique Zas. "Cherenkov radio pulses from electromagnetic showers in the time-domain". In: *Phys. Rev. D* 81 (2010), p. 123009. DOI: 10.1103/PhysRevD.81.123009. arXiv: 1002.3873 [astro-ph.HE].

[14] E. Zas, F. Halzen, and T. Stanev. "Electromagnetic pulses from high-energy showers: Implications for neutrino detection". In: *Phys. Rev. D* 45 (1992), pp. 362–376. DOI: 10.1103/PhysRevD.45.362.

[15] Daniel Garcia-Fernandez et al. "Calculations of electric fields for radio detection of ultrahigh energy particles". In: *Phys. Rev. D* 87.2 (2013), p. 023003. DOI: 10.1103/PhysRevD.87.023003. arXiv: 1210.1052 [astro-ph.HE].

[16] Sergio Sciutto. *AIRES User's Manual and Reference Guide; version 19.04.00*. http://aires.fisica.unlp.edu.ar/.

[17] Sergio Sciutto and Matias Tueros. *ZHAIReS User's Manual and Reference Guide*. http://www.fisica.unlp.edu.ar/zhaires.

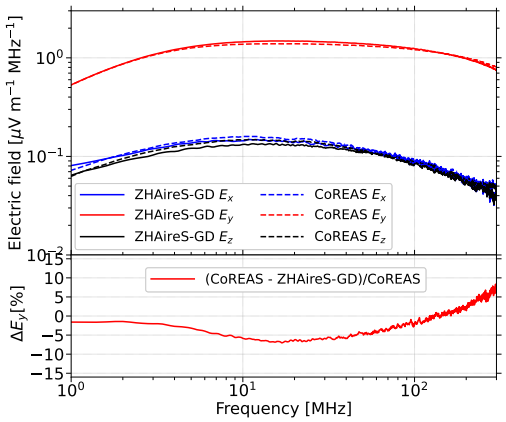

Antenna at $r = 277.8$ m north.

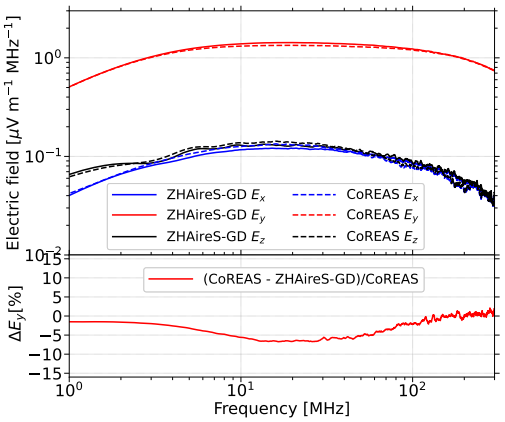

Antenna at $r = 277.8$ m south.

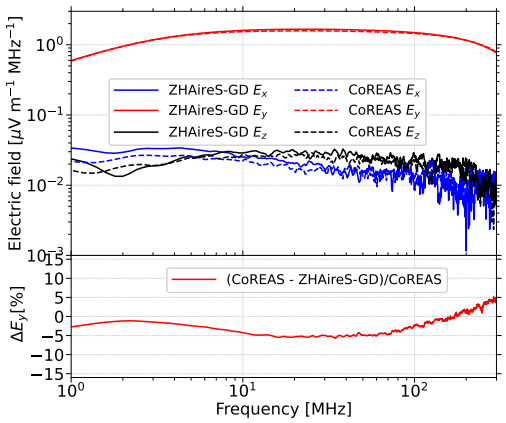

Antenna at $r = 166.7$ m east.

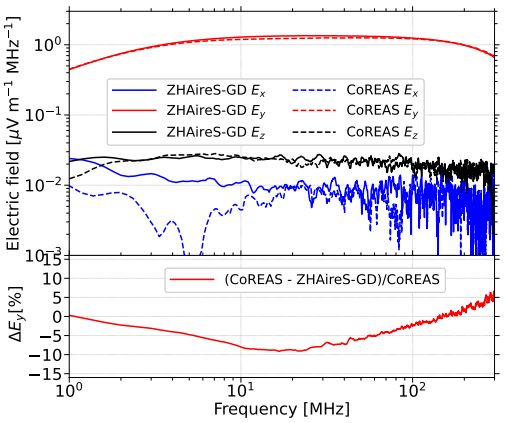

Antenna at $r = 166.7$ m west.

Figure 1: Frequency spectrum of the Fourier components of the electric field E_x (blue), E_y (red) and E_z (black) for observers on the ground close to the *Cherenkov ring*, as indicated in the captions of the panel. The labels in each panel indicate the cardinal directions: northwards (top left panel), southwards (top right panel), eastwards (bottom left panel), and westwards (bottom right panel) relative to the shower core. The Fourier components were obtained from simulations using ZHAireS (solid lines) and CoREAS (dashed lines) for 10^{17} eV iron-induced showers at $\theta = 45°$, propagating from north to south. The shower is moving from north to south, corresponding to azimuth angles of $\varphi_{\text{CoREAS}} = 180°$ in the CoREAS coordinate system and $\varphi_{\text{ZHAireS}} = 0°$ in the ZHAireS coordinate system. We used a horizontal magnetic field configuration $|\vec{B}| = 50\,\mu$T pointing to the magnetic north, so that $\sin\alpha \simeq 0.7$. The two showers compared were chosen from a sample of simulated showers so that the X_{max} values are similar: $X_{\text{max}}(\text{CoREAS}) = 566.1\,\text{g/cm}^2$ and $X_{\text{max}}(\text{ZHAireS}) = 566.6\,\text{g/cm}^2$. The bottom panels show the relative difference $\Delta E_y =$ (CoREAS−ZHAireS-GD)/CoREAS (in %) of the E_y component shown in the corresponding top panels.

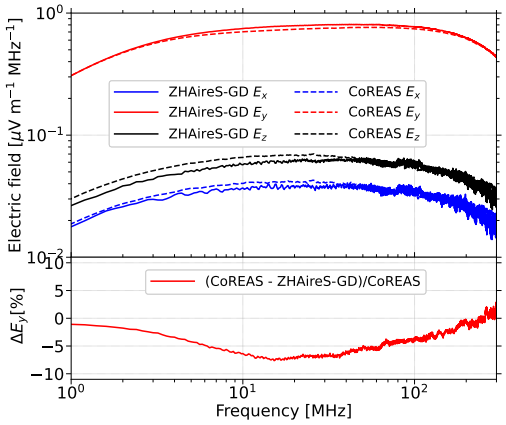

Antenna at r = 500 m north.

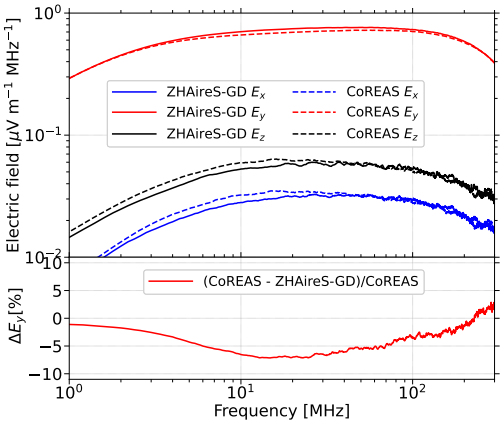

Antenna at r = 500 m south.

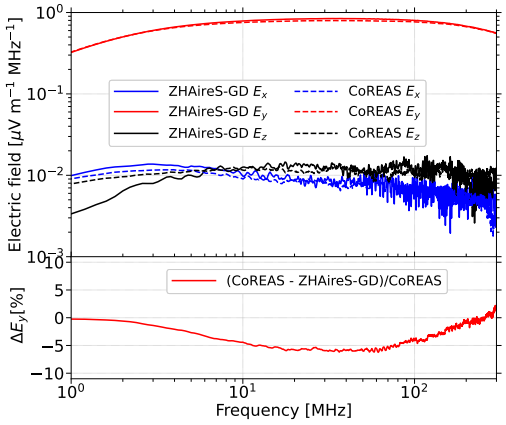

Antenna at r = 277.8 m east.

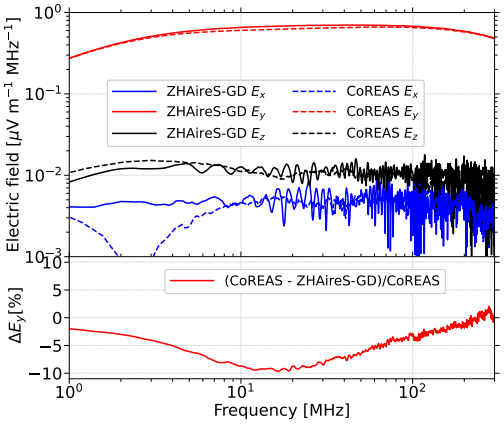

Antenna at r = 277.8 m west.

Figure 2: Same as Fig. 1 for showers with $\theta = 60°$ and observers at distances from the core of the shower on the ground, near the *Cherenkov ring*, as specified in the captions. We used a horizontal magnetic field configuration $|\vec{B}| = 50\,\mu$T pointing to the magnetic north, so that $\sin\alpha = -0.5$. The two showers compared were chosen from a sample of simulated showers so that the $X_{\max}$ values are similar: $X_{\max}$(CoREAS) = 584.3 g/cm^2 and $X_{\max}$(ZHAireS) = 585.0 g/cm^2. The bottom panels show the relative difference (in %) of the E_y component shown in the corresponding top panels.

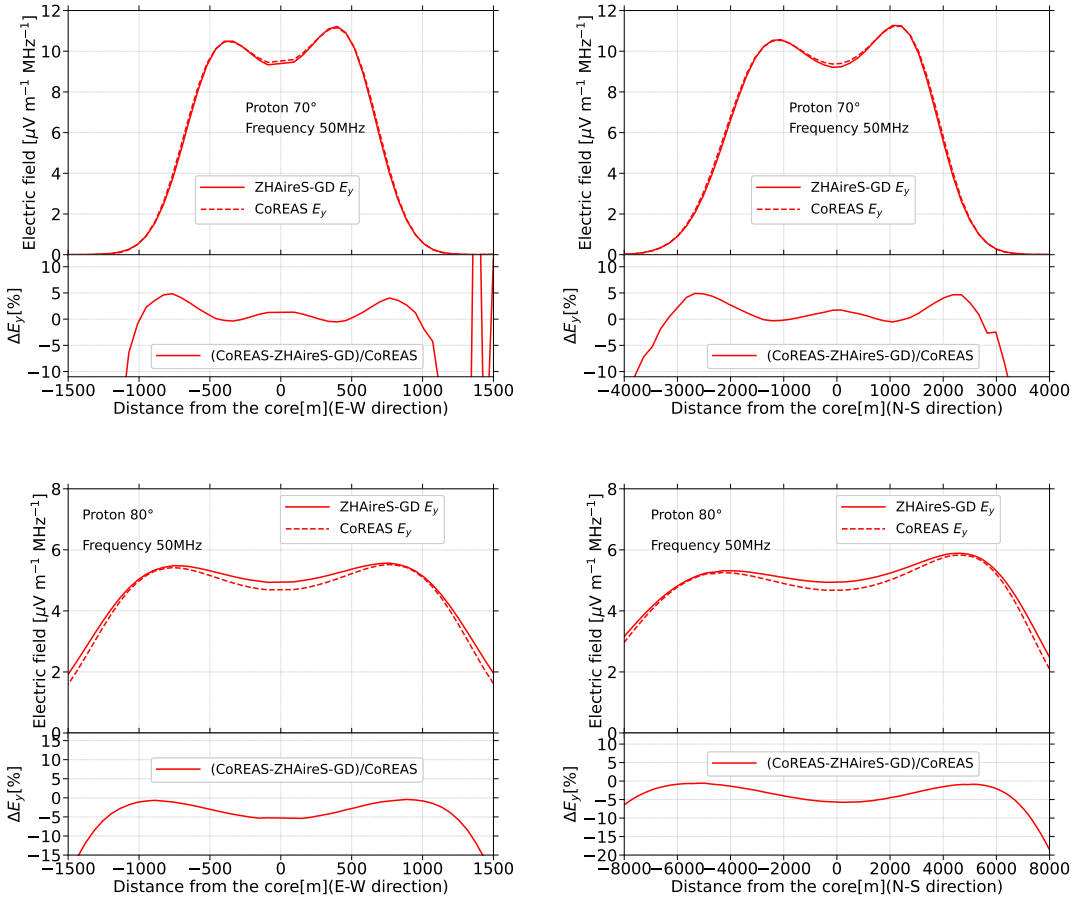

Figure 3: Modulus of the E_y component of the Fourier transform of electric field at frequency 50 MHz for observers at different distances from the shower core located along the north-south (NS) and east-west (EW) directions. The bottom panels show the relative difference ΔE_y = (CoREAS−ZHAireS-GD)/CoREAS (in %). Positive coordinates correspond to the antenna positions located north (or east) of the shower core. The simulations corresponds to proton showers at 10^{18} eV with zenith angle $\theta = 70°$ (top) and $\theta = 80°$ (bottom). The showers develop from north to south corresponding to azimuth angles $\varphi_{\text{CoREAS}} = 180°$ and $\varphi_{\text{ZHAireS}} = 0°$. We used a vertical magnetic field configuration with $|\vec{B}| = 50\,\mu$T, perpendicular to ground and pointing to the magnetic north, so that $\sin\alpha = 0.94$ for $\theta = 70°$ and $\sin\alpha = 0.98$ for $\theta = 80°$. The simulations were chosen from a sample of simulated showers so that their X_{max} values are very similar: $X_{\text{max}}(\text{ZHAireS}, \theta = 70°) = 718.8\,\text{g/cm}^2$ and $X_{\text{max}}(\text{CoREAS}, \theta = 70°) = 718.1\,\text{g/cm}^2$, while $X_{\text{max}}(\text{ZHAireS}, \theta = 80°) = 689.3\,\text{g/cm}^2$ and $X_{\text{max}}(\text{CoREAS}, \theta = 80°) = 690.5\,\text{g/cm}^2$.